

See discussions, stats, and author profiles for this publication at: <https://www.researchgate.net/publication/259804524>

# Artificial Sensing Intelligence with Silicon Nanowires for Ultra-Selective Detection in the Gas Phase.

ARTICLE *in* NANO LETTERS · JANUARY 2014

Impact Factor: 13.59 · DOI: 10.1021/nl404335p · Source: PubMed

CITATIONS

33

READS

105

## 4 AUTHORS:



**Bin Wang**

Technion - Israel Institute of Technology

13 PUBLICATIONS 305 CITATIONS

SEE PROFILE



**John C Cancilla**

Complutense University of Madrid

28 PUBLICATIONS 119 CITATIONS

SEE PROFILE



**Jose S. Torrecilla**

Complutense University of Madrid

127 PUBLICATIONS 1,825 CITATIONS

SEE PROFILE



**Hossam Haick**

Technion - Israel Institute of Technology

158 PUBLICATIONS 4,440 CITATIONS

SEE PROFILE

# Artificial Sensing Intelligence with Silicon Nanowires for Ultrasensitive Detection in the Gas Phase

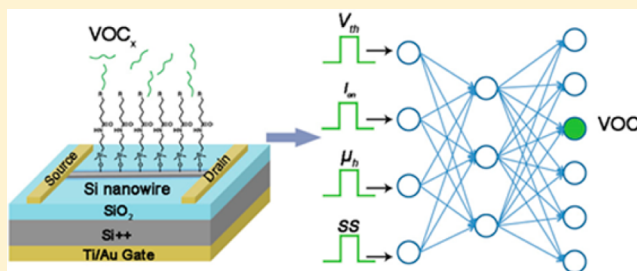
Bin Wang,<sup>†</sup> John C. Cancilla,<sup>‡</sup> Jose S. Torrecilla,<sup>‡</sup> and Hossam Haick<sup>\*,†</sup>

<sup>†</sup>Department of Chemical Engineering and Russell Berrie Nanotechnology Institute, Technion-Israel Institute of Technology, Haifa 3200003, Israel

<sup>‡</sup>Department of Chemical Engineering, Complutense University of Madrid, Madrid 28040, Spain

**S** Supporting Information

**ABSTRACT:** The use of molecularly modified Si nanowire field effect transistors (SiNW FETs) for selective detection in the liquid phase has been successfully demonstrated. In contrast, selective detection of chemical species in the gas phase has been rather limited. In this paper, we show that the application of artificial intelligence on deliberately controlled SiNW FET device parameters can provide high selectivity toward specific volatile organic compounds (VOCs). The obtained selectivity allows identifying VOCs in both single-component and multicomponent environments as well as estimating the constituent VOC concentrations. The effect of the structural properties (functional group and/or chain length) of the molecular modifications on the accuracy of VOC detection is presented and discussed. The reported results have the potential to serve as a launching pad for the use of SiNW FET sensors in real-world counteracting conditions and/or applications.



**KEYWORDS:** Field effect transistor, sensor, artificial neural network, selective, volatile organic compound, vapor

Silicon nanowire field effect transistors (SiNW FETs) are emerging as promising candidates for signal transduction and recognition of (bio)chemical species.<sup>1–10</sup> SiNW FETs provide several advantages over other sensing strategies, attributed to the methodical controllability over the sensing signals by means of gate voltages,<sup>11,12</sup> the ability to provide multiple device features to evaluate sensing signals,<sup>13</sup> the low power consumption of the SiNW FET, and to the extreme miniaturization features of the device dimensions.<sup>1,5</sup>

Implementation of the SiNW FETs for selective detection in liquid phase has been demonstrated. Functionalization of the Si NWs with amine/oxide,<sup>5</sup> biotin,<sup>6</sup> antigen,<sup>7</sup> or calmodulin<sup>5</sup> has allowed real-time selective (or specific) detection of pH, streptavidin, antibody, and calcium ions, respectively, in a liquid phase. Also, functionalization of SiNW FETs with tyrosine kinase,<sup>8</sup> antibody receptor,<sup>9</sup> or peptide nucleic acids (PNAs)<sup>10</sup> allowed selective detection of Ab1 tyrosine kinase, influenza-A virus, or DNA, respectively, in biological samples. In these applications, the receptors attached to the SiNW's surface bind specifically with the targeted (bio)molecule of interest, mostly through the "lock-and-key" approach,<sup>14,15</sup> and transduced via the FET platform as a change in the electrical signal(s).

In contrast to the liquid phase, it has been a challenge to obtain selective SiNW FET sensors for gaseous chemical species, such as, volatile organic compounds (VOCs) that are associated with environmental pollution, quality control, explosive materials, or various diseases.<sup>4,16–22</sup> As an intermediate way to increase the selectivity toward a specific VOC

of interest, arrays of cross-reactive (that is, semiselective) sensors in conjugation with pattern recognition methods have been utilized.<sup>4,17,23–30</sup> This approach mimics the human olfactory system and is often referred to as "electronic nose".<sup>4,17,23,25</sup> Excellent progress in the electronic nose field has been achieved during the past two decades but increased selectivity remains elusive, especially when the targeted VOC exists in an environment that includes counteracting contaminants or VOCs. Theoretically, increasing the number of the cross-reactive sensors in the array might lead to some improvements in the selectivity.<sup>4</sup> Nevertheless, increasing the number of sensors increases the power consumption and complicates the device circuitry and the related computation parts. Additionally, the higher the number of the sensing elements, the higher the risk of overfitting toward the analyzed data (i.e., cases where the applied algorithm describes random errors or noise instead of the underlying relationship),<sup>31</sup> particularly in cases where the sample size is limited.

Here, we present an approach that allows highly accurate selective detection as well as estimation of VOC(s) concentrations in both single-component and multicomponent mixtures. The approach relies on the use of multiple independent parameters of a specific molecularly modified SiNW FET (e.g., voltage threshold,  $V_{th}$ , hole mobility,  $\mu_h$ ,

**Received:** November 21, 2013

**Revised:** January 9, 2014

**Published:** January 17, 2014

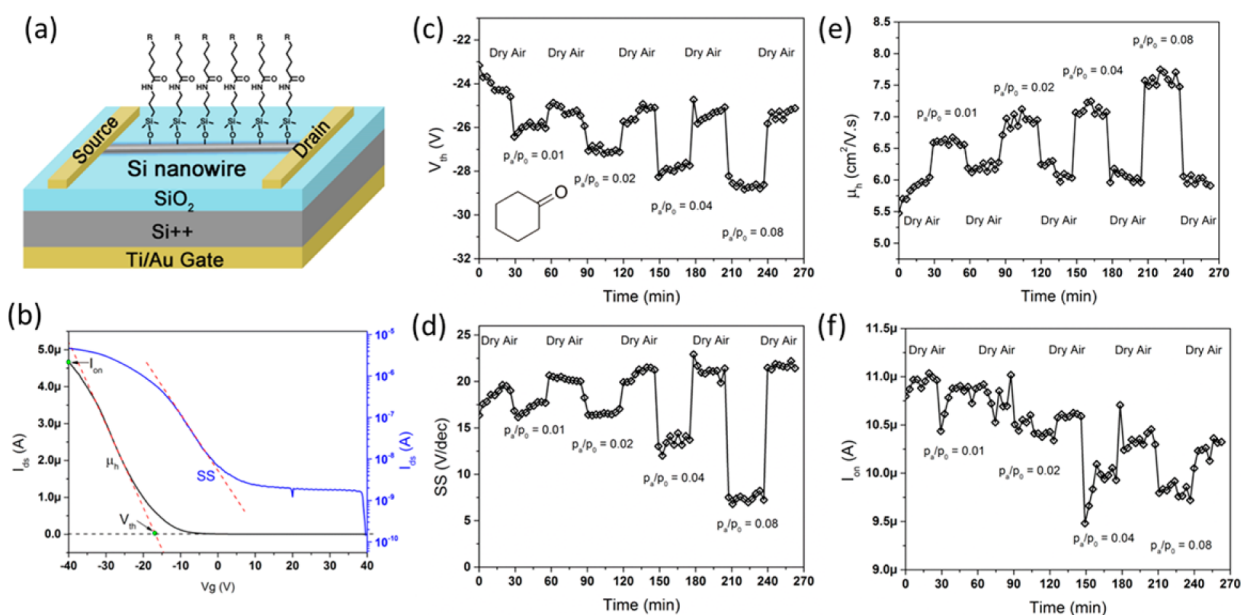
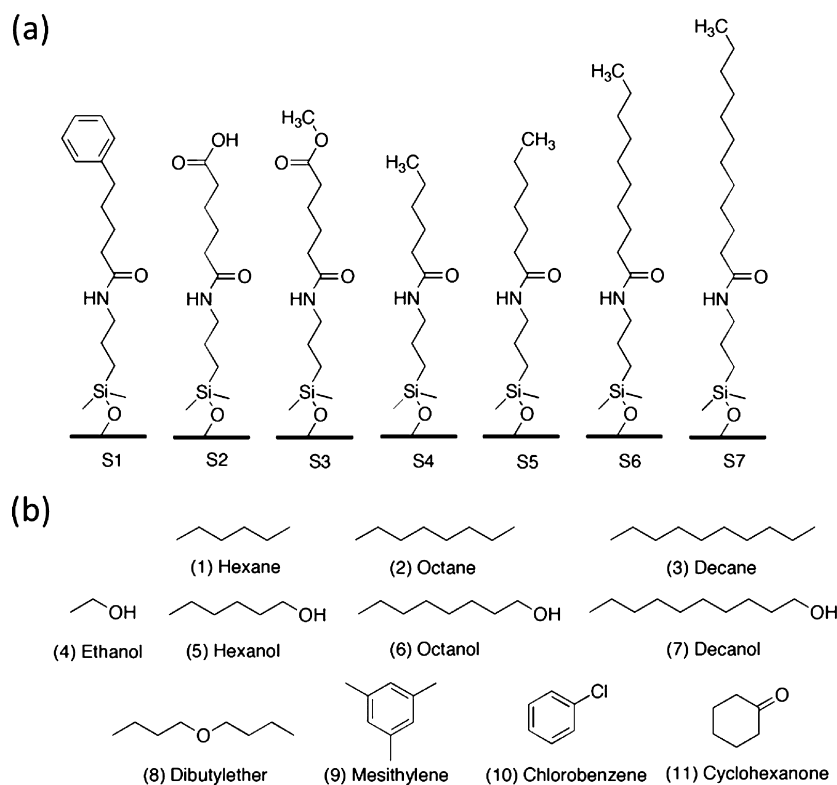


**Figure 1.** (a) Scheme of a molecularly modified SiNW FET sensor. (b) A typical linear (black line) and logarithmic scale (blue line)  $I_{ds}$ – $V_g$  curves of a SiNW FET. The sensing parameters are marked in the figure. Time-dependent response as expressed by (c)  $V_{th}$ , (d) SS, (e)  $\mu_h$ , and (f)  $I_{on}$  of sensor S4 on exposure to cyclohexanone at different concentrations ( $p_a/p_o$ ).

**Scheme 1. Structure of (a) Molecular Layers Attached to SiNW Surface(s) and (b) VOCs Used in This Study<sup>a</sup>**



<sup>a</sup>VOC-1, VOC-2, VOC-3, and VOC-9 are nonpolar chemicals, while the rest of VOCs are polar chemicals.

subthreshold swing (SS))<sup>1–3,13,32</sup> as input for artificial neural network (ANN) models,<sup>33,34</sup> which, in turn, can be trained in its ensemble to make the targeted detection. The effect of the device parameters as well as the effect of the molecular modifications on the obtained selectivity are presented and discussed.

Back-gate FETs with well-aligned SiNWs<sup>35,36</sup> in the channel are fabricated as described in the Supporting Information and illustrated in Figure 1a.<sup>11,12</sup> To detect VOCs, the channels of these devices (the SiNWs) are then coated with two series of silane monolayers (Scheme 1a). The first series of monolayers include similar backbones but different functional (head) groups (S1–S4). The head groups of S1 and S4 are electron-

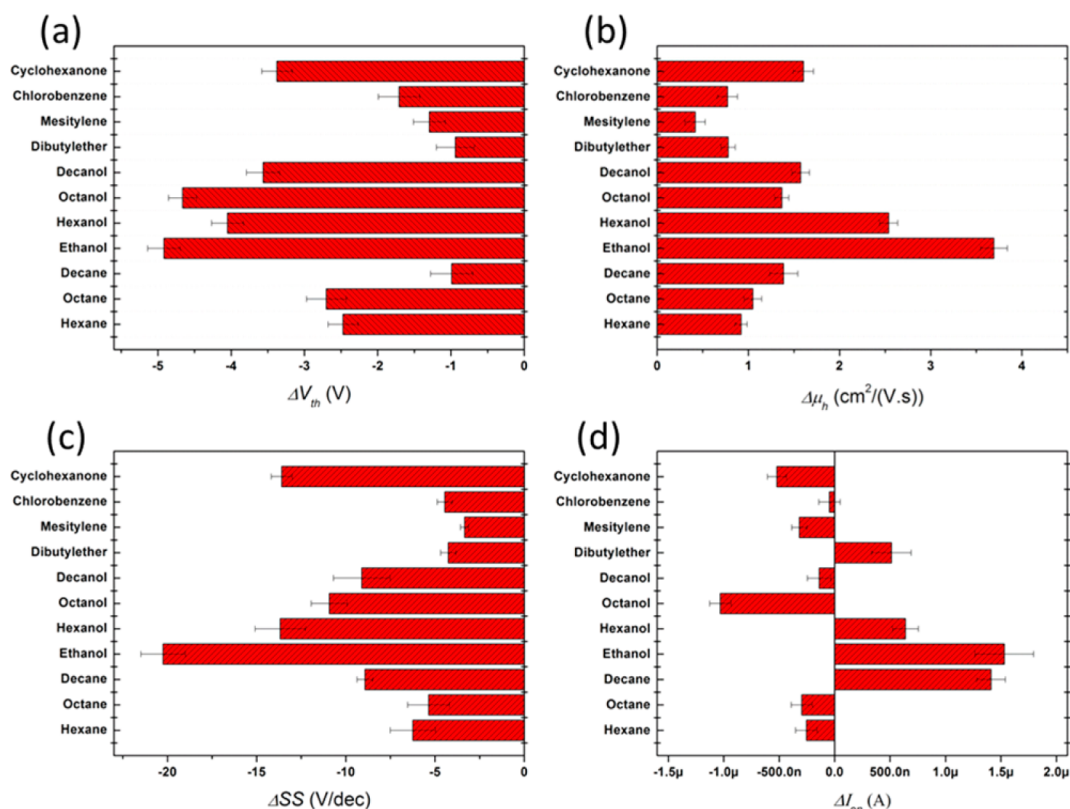


**Figure 2.** Changes in (a)  $V_{th}$  (b)  $\mu_h$  (c) SS, and (d)  $I_{on}$  of sensor S4 on exposure to various VOCs at concentration of  $p_a/p_o = 0.08$ .

donating, while those of S2 and S3 are electron-withdrawing (cf. ref 37). This series of monolayers are helpful for evaluating the effect of head groups in the sensing process.<sup>12</sup> The second series of monolayers include molecules with the same head groups ( $\text{CH}_3$ ) but with different chain lengths. This series of monolayers are helpful for evaluating the effect of the chain length on the sensing process (S4–S7).<sup>11</sup> X-ray photoelectron spectroscopy (XPS) and ellipsometry characterization of the applied molecular layers are presented and discussed in the Supporting Information. All molecularly modified SiNW FETs are loaded into a steel chamber with volume of  $\sim 170 \text{ cm}^3$  and simultaneously exposed to a series of eleven VOCs that are divided as follows: alkanes (VOC-1 to VOC-3), alcohols (VOC-4 to VOC-7), ethers (VOC-8), benzenes (VOC-9 and 10), and ketones (VOC-11); see Scheme 1b. Dry airflow and VOC flow with a 5 L/min constant flowrate are alternately introduced into the chamber. Signals are collected for 30 min under airflow, preceded by 30 min under flowing VOC vapor. Four successively increasing concentrations of each VOC:  $p_a/p_o = 0.01, 0.02, 0.04$  and  $0.08$ , are tested (where  $p_a$  and  $p_o$  stand for the VOC's partial pressure and vapor pressure, respectively, at a given temperature). Source-drain current ( $I_{ds}$ ) versus  $V_g$  curves (at  $V_{ds} = 2 \text{ V}$ ) are carried out during the exposure experiment (the  $V_g$  ranged from  $+40$  to  $-40 \text{ V}$ ).

Relying on the  $I_{ds}$  versus  $V_g$  curves obtained, the values of  $V_{th}$ ,  $\mu_h$ , and  $I_{on}$  (defined as  $I_{ds}$  at  $V_g = -40 \text{ V}$ ) of all sensors and VOCs are calculated, as described in the Supporting Information and illustrated in Figure 1b. The SS values are calculated from the  $\log(I_{ds})$  versus  $V_g$  curves. Figure 1c–f present time-dependent sensing parameters of S4 on exposure to cyclohexanone, as a representative example. As seen in the figures,  $V_{th}$ , SS, and  $I_{on}$  exhibit negative responses, while  $\mu_h$  exhibits positive responses on exposure to cyclohexanone. In

addition, the response amplitude of all the sensing parameters examined increases as the concentration of cyclohexanone increases. The response in  $V_{th}$  refers to the dipole moment change(s) surrounding the SiNWs, while the response in  $\mu_h$  is associated with the change of surface charge density of the SiNWs.<sup>11,12</sup>

Each molecularly modified SiNW FET has shown responses to a wide variety of VOCs. As a representative example, Figure 2 presents the responses of sensor S4 on exposure to eleven VOCs at  $p_a/p_o = 0.08$ . As shown in the figure, sensor S4 exhibits negative responses in  $V_{th}$  and SS, while it shows positive responses in  $\mu_h$  to all tested VOCs. In the  $I_{on}$  response plot, S4 shows positive responses to decane, ethanol, hexanol, and dibutylether and negative responses to the rest of the VOCs. These multiple sensing responses by each molecularly modified SiNW FET create a fingerprint for each VOC, which can then be used for VOC discrimination.

Relying on the raw responses of each SiNW FET sensor, ANN models<sup>31,32</sup> are employed to seek selectivity toward specific VOCs. The applied ANN is a feed-forward multilayer perceptron (MLP) with three layers: input, hidden, and output (Figure 3a). The four sensing parameters of each SiNW FET ( $V_{th}$ ,  $\mu_h$ ,  $I_{on}$ , and SS) at VOC concentration of  $p_a/p_o = 0.08$  are used as input nodes of the MLP. All correlation coefficient values between the sensing parameters used are lower than 0.1. Therefore, these four FET parameters are independent of each other. The eleven VOCs are encoded with dependent vectors in a ten-dimensional space and are set as the output layer of the ANN. Octanol is encoded as the original point of the ten-dimensional space, so a “0” is assigned to each element of its vector (see Supporting Information, Table S1). For the rest of the VOC encoding vectors, only one of the 10 elements is assigned a “1”, where the location of “1” is used to define VOC

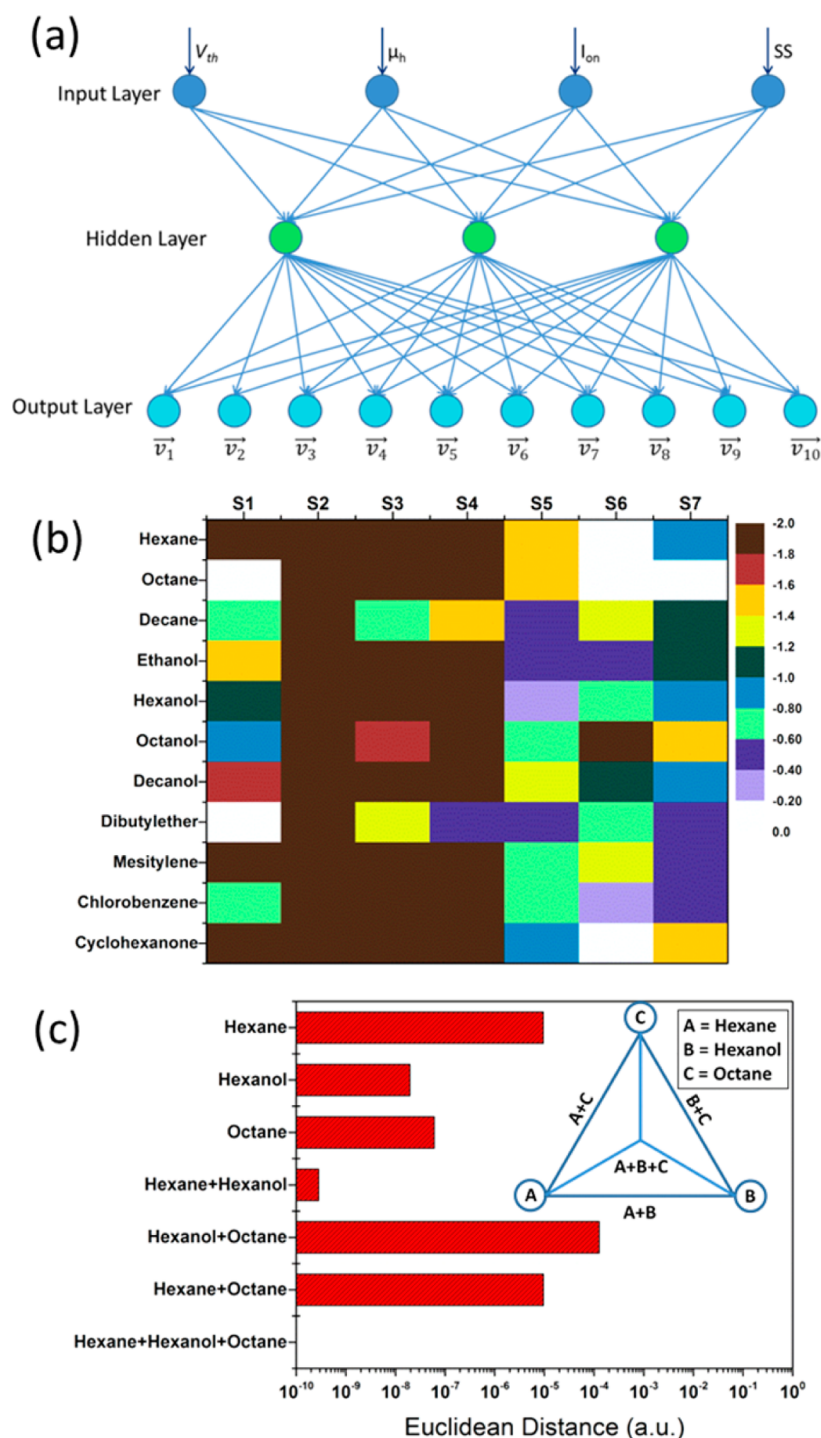


**Figure 3.** (a) Schematic illustration of an ANN model for VOC recognition. (b) Hot plots of logarithm Euclidean distance at VOC concentration of  $p_a/p_o = 0.08$ . (c) Euclidean distance of ANN outputs using sensor S3 to identify hexane, hexanol, octane, and their binary and ternary mixtures. All the tested VOC concentrations are at  $p_a/p_o = 0.08$ . Inset: Schematics of the relationship among single VOCs and their binary and ternary mixtures in ANN outputs.

species (see Supporting Information, Table S1). The rest are assigned “0”s. For instance, hexane and hexanol are characterized by the (0, 1, 0, 0, 0, 0, 0, 0, 0, 0) and (0, 0, 0, 0, 0, 0, 0, 0, 0, 1) vectors, respectively. The sigmoid function, which offers normalized results in the range of 0 to 1, is used as the transfer function of the applied ANN. The database obtained from tested SiNW FETs is split into two data sets, the learning data set (603 data points) and the verification (blind) data set (106 data points). First, the ANN models are trained

and optimized using the learning data set. ANN parameters, including the hidden neuron number (HNN), the Marquardt adjustment parameter ( $L_c$ ), the decrease factor for  $L_c$  ( $L_{cd}$ ), and the increase factor for  $L_c$  ( $L_{ci}$ ) are optimized to achieve more accurate output results (see Supporting Information, Table S2). To avoid overfitting effects and to improve the generalization capability of the model, small network topologies are selected and the trainBR training function is used. After the



training process concludes, verification data sets are used to test the ANN.

Prediction vectors of VOCs with each element value from 0 to 1 are generated from the verification data set test (see Supporting Information, Table S3–S9). For sensors S2–S5, the results show that each SiNW FET examined could recognize all eleven VOCs. On the other hand, S1 fails to recognize octane and dibutylether; S6 fails to recognize hexane, octane, and cyclohexanone; and S7 fails to recognize octane. The failures can be understood as the cases where the prediction vector position is incorrectly deviated from the target vector position. Thus, the Euclidean distance (ED; eq 1), the distance between the target vector and prediction vector, can be used to evaluate the recognition power of the sensors:

$$ED = \sqrt{\sum_{i=1}^k (X_i - Y_i)^2} \quad (1)$$

where  $X_i$  is the element of the target vector,  $Y_i$  is the element of the prediction vector, and  $k$  is the element number of the vector. It can be inferred that the smaller the ED, the more accurate the prediction value.

To better present the ED difference of the SiNW FET sensors examined, logarithms are taken from the ED values of each sensor and the results are plotted in Figure 3b. Among sensors with different functional groups (S1–S4), S2 (molecular chain with COOH functional group) shows the best performance for recognizing the tested VOCs. In contrast, S1 (molecular chain with phenyl functional group) shows the worst recognition of the tested VOCs, especially the uncyclic VOCs (alkanes, alcohols, and dibutylether). This might be attributed to the low adsorption ability of the uncyclic compounds in/on the phenyl ending groups.<sup>11</sup> The weak sensing responses of S1 lead to large classification errors and fail to identify VOCs. For the sensors with different alkyl chain length (S4–S7), the sensors with shorter alkyl chains show, in almost every case, better VOC recognition accuracy, compared with longer alkyl chains. Though the responses in  $V_{th}$  increase with the chain length of the molecular layer modifications,<sup>12</sup> the sensor recognition power for VOCs does not increase with this chain length. These facts suggest that the selectivity of SiNW FET sensors does not depend on a single sensing parameter. Rather, the selectivity depends on the difference in the combination of the four sensing parameters analyzed.

The selectivity achieved with one ANN-linked SiNW FET is not limited for VOCs in controlled or single-component medium only. Rather, this approach shows excellent selectivity toward specific VOC(s) in multicomponent mixture(s), even mixtures that contain counteracting compounds that have similar structures or physical/chemical properties to those of the target VOC. To demonstrate this feature, the four sensing parameters of S2 are measured on exposure to hexane, octane, hexanol, and their binary and ternary mixtures as well as being used as inputs of a new ANN model. Hexane, hexanol, and octane are encoded, respectively, with three dichotomical output vectors: (1,0,0), (0,1,0) and (0,0,1). The binary VOC mixtures of hexane and hexanol, hexane and octane, and hexanol and octane are characterized by (1,1,0), (1,0,1), and (0,1,1). The output of the ternary mixture is encoded with (1,1,1). As shown in Figure 3c, ED values of all tested samples are below  $10^{-3}$ . By a combination of multisignals from one SiNW FET sensor and ANN model, each of the VOCs in the tested mixture is perfectly identified. More important, the

trained ANN model successfully predicts if a certain VOC exists in a binary and even ternary VOC mixture. This result suggests that the combination of multiple signals from one SiNW FET and ANN models (i.e., without the need for array of different sensors, such as in the traditional electronic nose approach) allows identifying single VOCs and also certain VOC species in binary and ternary mixtures. Following further research and development, selective detection of specific VOCs in even more complex mixtures can be expected.

The combination between the SiNW FET and the ANN is found to be useful for estimating the VOC concentrations, too. The topology of the ANN for this purpose is similar to that of the VOC classifying model but differs in its output layer. Here, the output is used to estimate the VOC concentration. The optimization of this ANN is carried out by an experimental design based on the Box-Wilson Central Composite Design  $2^{4+}$ star points. This process leads to the selection of the ANN parameters that provide the ANN with the least mean prediction error (MPE) possible. Using the optimized ANN parameters, optimal estimation of each VOC concentration is obtained with lowest MPE. The MPE in relation to the eleven VOCs is summarized in Table 1 and the lowest MPEs of each

**Table 1.** MPEs of the Optimized ANN for All SiNW FET Sensors and VOCs

VOC	MPE (%)						
	S1	S2	S3	S4	S5	S6	S7
hexane	5.7	5.4	<b>&lt;0.1</b>	5.3	4.8	4.4	3.7
octane	4.7	1.1	<b>0.2</b>	0.9	4.9	1.3	8.7
decane	2.8	2.2	1.3	2.9	3.9	1.9	<b>0.8</b>
ethanol	3.9	0.4	<b>0.1</b>	2.9	4.2	1.7	0.3
hexanol	2.1	2.4	2.4	0.1	0.3	1.1	<b>&lt;0.1</b>
octanol	2.7	1.5	2.4	1.9	2.3	2.2	<b>1.4</b>
decanol	1.7	3.1	0.7	<b>0.1</b>	2.2	1.2	3.8
dibutylether	3.2	5.7	2.7	1.5	<b>&lt;0.1</b>	1.3	3.9
mesitylene	5.1	3.6	<b>0.7</b>	9.6	4.1	3.1	9.7
chlorobenzene	1.8	1.9	3.2	<b>0.5</b>	5.4	1.5	6.0
cyclohexanone	2.9	1.9	2.3	0.5	<b>&lt;0.1</b>	1.3	1.9

VOC are in bold. The results show that a combination of various device parameters from molecularly modified SiNW FETs and ANNs are able to estimate the concentration of all tested VOCs. As shown in the table, all tested SiNW FET sensors can be used individually to estimate VOC concentration with MPEs lower than 10%. In particular, S2 presents the best ANN performance in the estimation of the concentration of nonpolar VOCs (alkanes and mesitylene) concentration. On the other hand, SiNW FETs that are modified with methyl end groups show better estimation of the polar VOC concentrations. In this context, it is worth noting that testing concentration estimation power can be applied to screen qualified sensors for quantitative analysis.

In summary, we have developed a combined method that relies on SiNW FETs and ANN models to selectively recognize VOCs. By using only one SiNW FET sensor (rather than array of different sensors, as is the case in the traditional electronic nose approaches), 11 VOCs as well as their binary and ternary combinations could be perfectly recognized. The approach developed shows excellent selectivity toward specific VOC(s) in multicomponent mixture(s), even in mixture(s) that contain counteracting compounds with similar physical/chemical properties to those of the targeted VOC. Additionally, by

using ANNs with one SiNW FET, the VOC concentrations could be estimated with low errors. The quality or accuracy of “selective detection” is found to depend on the structural properties (functional group and/or chain length) of the molecular modifications. We believe the reported artificial sensing intelligence with SiNW FETs can be applied in other FET based sensors for selective VOC recognition and concentration prediction in multicomponent mixtures, as well as in real-world sensing applications in the gas phase.

## ■ ASSOCIATED CONTENT

### ● Supporting Information

Sensor preparation, N 1s XPS and ellipsometry surface characterization of the molecular modifications in S1–S7, target VOC output vectors of the ANNs, optimized ANN parameters, and output vectors of trained ANNs for applied SiNW FET sensors. This material is available free of charge via the Internet at <http://pubs.acs.org>.

## ■ AUTHOR INFORMATION

### Corresponding Author

\*E-mail: [hossam@tx.technion.ac.il](mailto:hossam@tx.technion.ac.il).

### Notes

The authors declare no competing financial interest.

## ■ ACKNOWLEDGMENTS

The research leading to these results has received funding from the FP7-Health Program under the LCAOS (Grant Agreement 258868). The authors acknowledge the Israel Council for Higher Education for partial support of Bin Wang's postdoctoral fellowship.

## ■ REFERENCES

- (1) Paska, Y.; Stelzner, T.; Assad, O.; Tisch, U.; Christiansen, S.; Haick, H. *ACS Nano* **2012**, *6*, 335–345.
- (2) Paska, Y.; Haick, H. *ACS Appl. Mater. Interfaces* **2012**, *4*, 2604–2617.
- (3) Paska, Y.; Stelzner, T.; Christiansen, S.; Haick, H. *ACS Nano* **2011**, *5*, 5620–5626.
- (4) Konvalina, G.; Haick, H. *Acc. Chem. Res.* **2014**, DOI: 10.1021/ar400070m.
- (5) Cui, Y.; Wei, Q. Q.; Park, H. K.; Lieber, C. M. *Science* **2001**, *293*, 1289–1292.
- (6) Duan, X.; Li, Y.; Rajan, N. K.; Routenberg, D. A.; Modis, Y.; Reed, M. A. *Nat. Nanotechnol.* **2012**, *7*, 401–407.
- (7) Stern, E.; Klemic, J. F.; Routenberg, D. A.; Wyrembak, P. N.; Turner-Evans, D. B.; Hamilton, A. D.; LaVan, D. A.; Fahmy, T. M.; Reed, M. A. *Nature* **2007**, *445*, 519–522.
- (8) Wang, W. U.; Chen, C.; Lin, K.-H.; Fang, Y.; Lieber, C. M. *Proc. Natl. Acad. Sci. U.S.A.* **2005**, *102*, 3208–3212.
- (9) Elnathan, R.; Kwiat, M.; Pevzner, A.; Engel, Y.; Burstein, L.; Khatchourints, A.; Lichtenstein, A.; Kantaev, R.; Patolsky, F. *Nano Lett.* **2012**, *12*, 5245–5254.
- (10) Hahm, J.-N.; Lieber, C. M. *Nano Lett.* **2004**, *4*, 51–54.
- (11) Wang, B.; Haick, H. *ACS Appl. Mater. Interfaces* **2013**, *5*, 2289–2299.
- (12) Wang, B.; Haick, H. *ACS Appl. Mater. Interfaces* **2013**, *5*, 5748–5756.
- (13) Ermanok, R.; Assad, O.; Zigelboim, K.; Wang, B.; Haick, H. *ACS Appl. Mater. Interfaces* **2013**, *5*, 11172–11183.
- (14) Du, Y.; Li, B.; Wang, E. *Acc. Chem. Res.* **2013**, *46*, 203–213.
- (15) Wolfgang, G. *Sens. Actuators, B* **1991**, *4*, 7–21.
- (16) Wallace, L. A. *Annu. Rev. Energy Environ.* **2001**, *26*, 269–301.
- (17) Broza, Y. Y.; Haick, H. *Nanomedicine* **2013**, *8*, 785–806.
- (18) Hakim, M.; Broza, Y. Y.; Barash, O.; Peled, N.; Phillips, M.; Amann, A.; Haick, H. *Chem. Rev.* **2012**, *112*, 5949–5966.
- (19) Tisch, U.; Haick, H. *Rev. Chem. Eng.* **2011**, *26*, 171–179.
- (20) Shuster, G.; Gallimidi, Z.; Reiss, A. H.; Dovgolevsky, E.; Billan, S.; Abdah-Bortnyak, R.; Kuten, A.; Engel, A.; Shiban, A.; Tisch, U.; Haick, H. *Breast Cancer Res. Treat.* **2011**, *126*, 791–796.
- (21) Peled, N.; Hakim, M.; Bunn, P. A., Jr.; Miller, Y. E.; Kennedy, T. C.; Mattei, J.; Mitchell, J. D.; Hirsh, F. R.; Haick, H. *J. Thorac. Oncol.* **2012**, *7*, 1528–1533.
- (22) Xu, Z. Q.; Ionsecu, R.; Broza, Y.; Tisch, U.; Ding, L.; Liu, H.; Song, Q.; Pan, Y. Y.; Xiong, F.-X.; Gu, K. S.; Sun, G. P.; Chen, Z.-D.; Leja, M.; Haick, H. *Br. J. Cancer* **2013**, *108*, 941–950.
- (23) Albert, K. J.; Lewis, N. S.; Schauer, C. L.; Sotzing, G. A.; Stitzel, S. E.; Vaid, T. P.; Walt, D. R. *Chem. Rev.* **2000**, *100*, 2595–2626.
- (24) Jurs, P. C.; Bakken, G. A.; McClelland, H. E. *Chem. Rev.* **2000**, *100*, 2649–2678.
- (25) Rakow, N. A.; Suslick, K. S. *Nature* **2000**, *406*, 710–713.
- (26) Haick, H.; Hakim, M.; Patrascua, M.; Levenberg, C.; Shehada, N.; Nakhoul, F.; Abassi, Z. *ACS Nano* **2009**, *3*, 1258–1266.
- (27) Peng, G.; Tisch, U.; Haick, H. *Nano Lett.* **2009**, *9*, 1362–1368.
- (28) Peng, G.; Trock, E.; Haick, H. *Nano Lett.* **2008**, *8*, 3631–3635.
- (29) Zilberman, Y.; Ionescu, R.; Feng, X.; Müllen, K.; Haick, H. *ACS Nano* **2011**, *5*, 6743–6753.
- (30) Zilberman, Y.; Tisch, U.; Shuster, G.; Pisula, W.; Feng, X.; Müllen, K.; Haick, H. *Adv. Mater.* **2010**, *22*, 4317–4320.
- (31) Hierlemann, A.; Gutierrez-Osuna, R. *Chem. Rev.* **2008**, *108*, 563–613.
- (32) Bayn, A.; Feng, X.; Müllen, K.; Haick, H. *ACS Appl. Mater. Interf.* **2013**, *5*, 3431–3440.
- (33) Torrecilla, J. S.; Tortuero, C.; Cancilla, J. C.; Díaz-Rodríguez, P. *Talanta* **2013**, *113*, 93–98.
- (34) Khan, J.; Wei, J. S.; Ringner, M.; Saal, L. H.; Ladanyi, M.; Westermann, F.; Berthold, F.; Schwab, M.; Antonescu, C. R.; Peterson, C.; Meltzer, P. S. *Nat. Med.* **2001**, *7*, 673–679.
- (35) Assad, O.; Leshansky, A. M.; Wang, B.; Stelzner, T.; Christiansen, S.; Haick, H. *ACS Nano* **2012**, *6*, 4702–4012.
- (36) Wang, B.; Stelzner, T.; Dirawi, R.; Assad, O.; Shehada, N.; Christiansen, S.; Haick, H. *ACS Appl. Mater. Interfaces* **2012**, *4*, 4251–4258.
- (37) Gozlan, N.; Haick, H. *J. Phys. Chem. C* **2008**, *112*, 12599–12601.